NASA Contractor Report 172129

ICASE

VISCOUS, RESISTIVE MHD STABILITY COMPUTED

BY SPECTRAL TECHNIQUES

R. B. Dahlburg

T. A. Zang

D. Montgomery

M. Y. Hussaini

Contract Nos. NAS1-15810 & NAS1-16394
Grant Nos. NAG1-109 & NSG-7416
March 1983

INSTITUTE FOR COMPUTER APPLICATIONS IN SCIENCE AND ENGINEERING
NASA Langley Research Center, Hampton, Virginia 23665

Operated by the Universities Space Research Association

National Aeronautics and
Space Administration

Langley Research Center
Hampton, Virginia 23665

VISCOUS, RESISTIVE MHD STABILITY COMPUTED BY SPECTRAL TECHNIQUES

R. B. Dahlburg, T. A. Zang, D. Montgomery
College of William and Mary

M. Y. Hussaini
Institute for Computer Applications in Science and Engineering

ABSTRACT

Expansions in Chebyshev polynomials are used to study the linear stability of one-dimensional magnetohydrodynamic (MHD) quasi-equilibria in the presence of finite resistivity and viscosity. The method is modeled on the one used by Orszag in accurate computation of solutions of the Orr-Sommerfeld equation. Two Reynolds-like numbers involving Alfvén speeds, length scales, kinematic viscosity, and magnetic diffusivity govern the stability boundaries, which are determined by the geometric mean of the two Reynolds-like numbers. Marginal stability curves, growth rates versus Reynolds-like numbers, and growth rates versus parallel wave numbers are exhibited. A numerical result which appears general in that instability has been found to be associated with inflection points in the current profile, though no general analytical proof has emerged. It is possible that nonlinear subcritical three-dimensional instabilities may exist, similar to those in Poiseuille and Couette flow.

The work for R. Dahlburg and D. Montgomery was supported in part by NASA Grant NSG-7416 and by U. S. D. O. E. Contract DE-AS05-76ET53045 at the College of William and Mary, Williamsburg, VA 23185. The work of T. A. Zang was suppoted by NASA Grant NAG-1-109 at the College of William and Mary, Williamsburg, VA 23185. The work of M. Y. Hussaini was supported by NASA Contracts No. NAS1-16394 and NAS1-15810 while the author was in residence at ICASE, NASA Langley Research Center, Hampton, VA 23665.

The linear stability of plane shear flows has been one of the most intensively studied hydrodynamic problems from the time of Rayleigh, since it was thought to hold clues to the nature of turbulence (see, e.g., Lin[1] or Maslowe[2]). Although the linear theory alone appears to be inadequate to predict the onset of shear flow instabilities, it remains an important first step in any discussion of the problem. We report here on an analogous problem in incompressible magnetohydrodynamics (MHD). We report numerical solutions of the quiescent-MHD analogue of the Orr-Sommerfeld equation, using spectral methods developed by Orszag[3].

We begin with the incompressible MHD equations in a familiar dimensionless form:

$$\frac{\partial \underset{\sim}{B}}{\partial t} = \nabla \times (\underset{\sim}{v} \times \underset{\sim}{B}) + \frac{1}{S} \nabla^2 \underset{\sim}{B} \ , \tag{1}$$

$$\frac{\partial \underset{\sim}{v}}{\partial t} = -\underset{\sim}{v} \cdot \nabla \underset{\sim}{v} + \underset{\sim}{B} \cdot \nabla \underset{\sim}{B} - \nabla p + \frac{1}{M} \nabla^2 \underset{\sim}{v} \ , \tag{2}$$

supplemented by the conditions that $\nabla \cdot \underset{\sim}{v} = 0$ and $\nabla \cdot \underset{\sim}{B} = 0$. $\underset{\sim}{B}$ is the magnetic field measured in units of a mean magnetic field magnitude $\bar{B}$, say. The velocity field is measured in units of the mean Alfvén speed $C_A \equiv \bar{B}(4\pi\rho)^{-1/2}$, where ρ is the mass density, assumed uniform. The dimensionless pressure is p, and it is determined by solving the Poisson equation which results from taking the divergence of Eq. (2) and using $\nabla \cdot \partial \underset{\sim}{v}/\partial t = 0$. The dimensionless numbers S and M have the structure of Reynolds numbers. $S \equiv C_A L/\eta$ is the Lundquist number, where η is the magnetic diffusivity and L is a macroscopic length scale; $M \equiv C_A L/\nu$ is a viscous analogue, where ν is a kinematic viscosity. Both η

and ν are assumed to be scalars. The regime of most interest is that in which S and M are both substantially greater than unity.

The boundary conditions are taken to be those appropriate to a perfectly-conducting, mechanically-impenetrable wall bounding a viscous, resistive magnetofluid: $\underset{\sim}{v} = 0$, $\hat{n} \cdot \underset{\sim}{B} = 0$, and $\hat{n} \times (\nabla \times \underset{\sim}{B}) = 0$, where $\hat{n}$ is the unit normal at the wall.

We study the linear stability of the quasi-equilibrium $\underset{\sim}{B}^{(o)} = (B_o(y),0,0)$ and $\underset{\sim}{v}^{(o)} = (0,0,0)$ between parallel, plane infinite boundaries at $y = 1$ and $y = -1$. The current density is in the z-direction only: $j_o = -DB_o$, where $D \equiv d/dy$. The configuration described is not a true equilibrium, and the magnetic field will resistively decay according to $B_o(y,t) = \exp(S^{-1}t\nabla^2)B_o(y,0)$. The temporal variation will be assumed to be slow enough to be negligible: $B_o(y,t) \cong B_o(y,0) = B_o(y)$. This implies that our stability boundaries will not be accurate in regions of small S; there is in this feature a conceptual difference from the already much studied[4,5,6] problem of a mean flow parallel to a uniform magnetic field with no current, which is a true equilibrium, and from Hartmann flow[6].

A linear expansion $\underset{\sim}{B} = \underset{\sim}{B}^{(o)} + \underset{\sim}{B}^{(1)}$, $\underset{\sim}{v} = \underset{\sim}{v}^{(1)}$, is assumed, with products of $\underset{\sim}{v}^{(1)}$ and $\underset{\sim}{B}^{(1)}$ being discarded everywhere in the equations of motion. Manipulating the components of the resulting linear equations, we may prove a Squire's theorem[1], which implies that for the location of the most unstable modes it suffices to consider the two-dimensional case: $\partial/\partial z$ may be set equal to zero throughout. All variations with the parallel coordinate x and the time t are assumed to be contained in a factor $\exp(i\alpha x - i\omega t)$, with α an arbitrary, real, parallel wave number and $\omega = \omega_r + i\omega_i$ a complex eigenvalue. Dahlburg and Montgomery[7] have given the eigenvalue equations in the form used here:

$$(D^2-\alpha^2)^2 v = -i\omega M(D^2-\alpha^2)v - i\alpha MB_o(D^2-\alpha^2)b + i\alpha M(D^2B_o)b \qquad (3)$$

and

$$(D^2-\alpha^2 + i\omega S)b = -i\alpha SB_o v. \qquad (4)$$

Here b and v are the y components of $\underset{\sim}{B}^{(1)}$ and $\underset{\sim}{v}^{(1)}$, and depend only upon y. The boundary conditions become $v = 0$, $Dv = 0$, and $b = 0$ at $y = 1$ and $y = -1$.

Equations (3) and (4) are the magnetostatic analogue of the Orr-Sommerfeld Equation, which in the same notation[1,2,3] is $(D^2-\alpha^2)^2 v = i\alpha R[(U_o-\omega/\alpha)(D^2-\alpha^2)v-(D^2U_o)v]$, where $U_o(y)$ is a shear flow velocity profile in the x direction, R is the Reynolds number, and the boundary conditions are that $v = 0$, $Dv = 0$ at $y = \pm 1$.

Equations (3) and (4) are quite similar to eigenvalue problems arising in connection with confinement of thermonuclear plasmas. The literature of "tearing modes" is extensive, and we may cite the central papers of Furth, Killeen, and Rosenbluth[8], of Wesson[9], of Coppi, Greene, and Johnson[10], of Furth, Rutherford, and Selberg[11], and of Dibiase and Killeen[12]. Concern has frequently been with the non-viscous ($M = \infty$) case, which lowers the order of the differential equations. Viscous results from a linear initial-value computation have been reported by Dibiase and Killeen[12] for the compressible case, and to the extent that the results can be compared, ours do not appear to disagree with theirs. Because for plasmas of interest to date, the calculated viscosity coefficients give estimates of ν at least as great as those for η (see, e.g., Braginskii[13]), it seems desirable to retain viscous effects even at the price of raising the order of the eigenvalue problem to the point where results can be extracted only numerically.

Analytical information is difficult to extract even for the simpler Orr-Sommerfeld equation (e.g., Maslowe[2] or Reid[14]) and numerical solution is

indicated here. We use a spectral technique closely patterned on the method used by Orszag[3] to calculate critical Reynolds numbers for Poiseuille flow to six-figure accuracy. It is to be expected that spectral methods will find further applications in plasma physics beyond the immediate ones.

The mean magnetic field $B_o(y)$ and the perturbation quantities v and b are expanded in truncated Chebyshev series

$$B_o(y) = \sum_{n=0}^{N} \tilde{B}_n T_n(y)$$

$$v(y) = \sum_{n=0}^{N} \tilde{v}_n T_n(y)$$

$$b(y) = \sum_{n=0}^{N} \tilde{b}_n T_n(y), \qquad (5)$$

where $T_n(y)$ is the n^{th} Chebyshev polynomial of the first kind, and $\tilde{B}_n$, $\tilde{v}_n$, $\tilde{b}_n$ are the respective expansion coefficients.

The equations satisfied by the (unknown) expansion coefficients are obtained by substituting the $N \to \infty$ expansions of (5) into Eqs. (3) and (4), each of which produces a countably infinite number of equations in the expansion coefficients for n = 0, 1, 2, ..., when the orthogonality and recursion relations[3] are used. We then set all coefficients beyond n = N to zero, use the n = 0 to n = N-4 equations from (3), the n = 0 to N-2 equations from (4), and the boundary conditions $\sum_{n=0}^{N} \tilde{v}_n = 0$, $\sum_{n=0}^{N} (-1)^n \tilde{v}_n = 0$, $\sum_{n=1}^{N} n^2 \tilde{v}_n = 0$, $\sum_{n=1}^{N} (-1)^n n^2 \tilde{v}_n = 0$, $\sum_{n=0}^{N} \tilde{b}_n = 0$, and $\sum_{n=0}^{N} (-1)^n \tilde{b}_n = 0$. This method of truncation is called the "tau approximation" after Lanczos[15]; Gottlieb and Orszag[16] give a general discussion of the use of the tau method in the Chebyshev case.

This spectral discretization process yields a generalized eigenvalue problem which can be written as $Ax = \omega Bx$, where the vector $x = (\tilde{v}_o, \tilde{v}_1, \ldots \tilde{v}_N, \tilde{b}_o, \tilde{b}_1, \ldots \tilde{b}_N)$, and A and B are non-symmetric (2N+2) by (2N+2) square matrices.

As is customary for this type of stability problem, either global or local methods are used to determine the eigenvalues. The global method is based on the QR algorithm (Wilkinson[17], Gary and Helgason[18]) and produces a full spectrum of eigenvalues. It is employed when no good guess for the least stable (or most unstable) eigenvalue is available. The local method employs inverse Rayleigh iteration[17] and converges to the eigenvalue (and its associated eigenfunction) closest to the initial guess for the eigenvalue. The global method may be used to identify the eigenvalue with the largest imaginary part, and the local method is useful when making a series of computations in which either the wavenumber or the Reynolds numbers are slowly varied.

For functions $B_o(y)$ which are antisymmetric about $y = 0$, it is readily inferred from Eqs. (3) and (4) that v and b are of opposite parity when reflected about $y = 0$. We have confined attention to the case $B_o(y) = -B_o(-y)$ with an associated current distribution $j_o = -DB_o$ which has even parity about $y = 0$: the classic "sheet pinch" configuration. This configuration (indeed, any $B_o(y)$ profile) can be rigorously proved to be stable in the ideal limit ($M = \infty$, $S = \infty$); any instabilities must result from finite values of S or M or (in our case) both.

We have solved for the several eigenfunctions corresponding to the largest values of ω_i for four different antisymmetric profiles $B_o(y)$:

$$B_o^{I}(y) \equiv y - y^3/3$$

$$B_o^{II}(y) \equiv \tan^{-1}\gamma y - \gamma y(\gamma^2+1)^{-1}$$

$$B_o^{III}(y) \equiv y - y^{21}/21$$

$$B_o^{IV}(y) \equiv \sinh^{-1}\gamma y - \gamma y(\gamma^2+1)^{-1/2}. \qquad (6)$$

Two numerical results have characterized all runs performed, and though we have been unable to prove either one analytically, we suspect they are generally true: (1) as S or M is raised a first unstable eigenvalue always appears ($\omega_i > 0$) at finite values of S and M with $\omega_r = 0$; and (2) a necessary condition that instabilities appear is that the current profile j_o shall have an inflection point between y = -1 and y = +1. Steep current gradients alone seem insufficient to produce instability. For example, $B_o^{III}(y)$, which has a large maximum current gradient of 20 near the walls, was found to be stable up to $M = 10^4$, $S = 10^4$ (for $\alpha = 1$), while profiles such as B_o^{II} which did contain inflection points would characteristically be unstable for S and M no greater than a few tens, with considerably smaller current gradients involved.

Particularly extensive investigations were carried out for the profile $B_o^{II}(y)$ for various values of α, S, M, and the "stretching parameter" γ. Figure 1 is a plot of $B_o^{II}(y)$ and its associated current profile $j_o^{II}(y) = -DB_o^{II}$ as a function of y for $\gamma = 10$. This case will be used to illustrate the results in Figs. 2 through 9.

Figure 2 shows typical eigenfunctions, stable and unstable, computed from the B_o^{II} of Fig. 1. Figure 2a applies to S = M = 10, for the least-damped eigenvalue $\omega_i = -0.1695$. For this case, $\omega_r = 0$, $\alpha = 1.0$, $b = ib_i$ is purely imaginary, and $v = v_r$ is purely real. This last property always applies to the eigenfunction with the greatest ω_i. Figure 2b shows b_i, v_r for an eigenfunction immediately above the instability threshold, with S = M = 20, $\omega_i = 0.06940$, $\alpha = 1.0$, $\omega_r = 0$. Figure 2c shows b_i, v_r well above the threshold, with S = M = 1000, $\alpha = 1.0$, $\omega_i = 0.19687$, and $\omega_r = 0$. Figure 2d shows the case S = 10, $M = 10^5$, with $\alpha = 1.0$, $\omega_i = 0.4397$ and $\omega_r = 0$. Figure 2e shows the case $S = 10^5$, M = 10, $\omega_i = 0.002537$, $\alpha = 1.0$, $\omega_r = 0$, and

illustrates the (perhaps unsurprising) result that viscosity is better at suppressing unstable growth than resistivity.

The damped modes have, in general, both ω_i and ω_r finite. Typical eigenfunctions for a highly damped mode for B_o^{II} are shown in Fig. 3 ($\omega_r = -0.40492$, $\omega_i = -6.01303$, $S = M = 20$, $\alpha = 1.0$).

At the stability threshold $\omega = 0$, the scaling $v' \equiv vM^{-1/2}$, $b' \equiv bS^{-1/2}$ reduces Eqs. (3) and (4) to a pair of equations for v' and b' which depend upon S and M only in the combination $\sqrt{SM}$ (and, of course, upon α). The neutral stability curve in the SM plane, across which ω_i becomes positive for some α, is therefore a hyperbola, approximately $SM = 231.9$. The computed location of this hyperbola (for B_o^{II} with $\gamma = 10$) is shown in Fig. 4. The relatively low values of the critical Reynolds numbers (two orders of magnitude or more below the corresponding hydrodynamic ones for shear flows) are perhaps the most significant feature of this graph. It is also interesting that for low enough values of either Reynolds number, stability will always result for any fixed value of the other, but since SM increases with temperature, according to kinetic theory estimates[13], at high enough temperatures, we may always expect to be on the unstable side of the boundary.

To make a comparison with traditional[1] hydrodynamic plots, Fig. 5 exhibits a set of marginal stability curves: $\omega = 0$ in the α, S plane for fixed M for B_o^{II} and $\gamma = 10$. The first unstable α (which, for the reasons previously noted, must be the same for all such curves) is $\alpha = \alpha_c = 1.184 \pm 0.005$. We have generated the same curves (not shown) in the α, M plane for fixed S.

Figure 6a shows a growth rate (ω_i vs. S) curve for $M = 10$. Figure 6b shows a logarithmic plot for large values of S, illustrating the $S^{-3/5}$ regime identified analytically by Furth et al[8]. Figure 7 shows the somewhat different behavior of ω_i vs. M for fixed S. Figure 8a shows a contour

plot of two periods of the magnetic field lines $\underset{\sim}{B}^{(0)} + \underset{\sim}{B}^{(1)}$ for the B_o^{II} equilibrium plus a 20 percent admixture of the eigenfuction shown in Fig. 2b. Figure 8b shows the streamlines of the velocity field for the same eigenfuction. Figure 9 shows the growth rate ω_i vs. α for several values of S and M.

The results presented have all been computational and are not the result of an asymptotic "tearing layer" analysis. The marginal stability curves such as Fig. 5 or the stability hyperbola of Fig. 4 could only have been obtained numerically. Despite these new results, we are well aware of other potentially important physical effects which have been left out of the analysis, such as compressibility, or the effects of spatially varying viscosity and resistivity tensors. Nevertheless, we believe there to be some value in bringing a more classical hydrodynamic perspective to bear on this highly idealized problem. It is not impossible that subcritical instability thresholds from nonlinear three-dimensional computations may be identified for this problem as they have been for shear flows (see, e.g., Orszag and Kells[19] or Orszag and Patera[20]). Further computations of a more elaborate kind will be required to test this possibility; for further discussion of the hydrodynamic antecedents, see the review by Herbert[21].

ACKNOWLEDGMENTS

Conversations with Drs. W. H. Matthaeus and G. Vahala are gratefully acknowledged.

REFERENCES

1. Lin, C. C. (1955) The Theory of Hydrodynamic Stability (Cambridge University Press, Cambridge, U.K.) Chs. 1 and 2.
2. Maslowe, S. A. (1981), in Hydrodynamic Instabilities and the Transition to Turbulence, ed. by Swinney, H. L., and Gollub, J. P. (Springer-Verlag, Berlin) pp. 181-228.
3. Orszag, S. A. (1971) J. Fluid Mech. 50, pp. 689-703.
4. Michael, D. H. (1953) Proc. Cambridge Phil. Soc. 49, 166-168.
5. Stuart, J. T. (1954) Proc. Roy. Soc. (London) A221, 189-206.
6. Betchov, R. and Criminale, W. O., Jr. (1967) Stability of Parallel Flows (Academic Press, New York). See in particular Chapter IX on "Magnetohydrodynamic Effects", pp. 198-215.
7. Montgomery, D. (1982), to be published in Spectral Methods in Fluid Mechanics, ed. by Gottlieb, D., Hussaini, M. Y., and Voigt, R. (SIAM, Philadelphia; to appear in 1983).
8. Furth, H. P., Killeen, J., and Rosenbluth, M. N. (1963) Phys. Fluids 6, pp. 459-484.
9. Wesson, J. (1966) Nucl. Fusion 6, pp. 130-134.
10. Coppi, B., Greene, J.M., and Johnson, J.L. (1966) Nucl. Fusion 6, pp. 101-117.
11. Furth, H. P., Rutherford, P. H., and Selberg, H. (1973) Phys. Fluids 16, pp. 1054-1063.
12. Dibiase, J. A., and Killeen, J. (1977), J. Comp. Phys. 24, pp. 158-185.

13. Braginskii, S. I. (1965), in Reviews of Plasma Physics, Vol. I, ed. by Leontovich, M.A. (Consultant's Bureau, New York) pp. 205-309.

14. Reid, W. H., (1965) in Basic Developments in Fluid Dynamics, ed. by Holt, M. (Academic Press, New York) pp. 249-307.

15. Lanczos, C. (1956) Applied Analysis (Prentice Hall, New York).

16. Gottlieb, D., and Orszag, S. A. (1977) Numerical Analysis of Spectral Methods: Theory and Application (SIAM, Philadelphia).

17. Wilkinson, J. H. (1965) The Algebraic Eigenvalue Problem (Oxford University Press, London).

18. Gary, J., and Helgason, R. (1970) J. Comp. Phys. 5, pp. 169-187.

19. Orszag, S. A., and Kells, L. C. (1980) J. Fluid Mech. 96, pp. 159-205.

20. Orszag, S. A., and Patera, T. (1980) Phys. Rev. Lett. 45, pp. 989-993.

21. Herbert, T. (1981) Stability of Plane Poiseuille Flow: Theory and Experiment. XV Symposium on Advanced Problems and Methods in Fluid Mechanics, Jachranka, Poland (to be published in Fluid Dynamics Transactions, Vol. II).

FIGURE CAPTIONS

Fig. 1 $B_o = B_o^{II}(y)$ and its associated current profile $j_o = -DB_o$, for $\gamma = 10$.

Fig. 2a Eigenfunctions $b = ib_i$, $v = v_r$ for the least-damped eigenvalues for $M = 10$, $S = 10$.

Fig. 2b Eigenfunctions $b = ib_i$, $v = v_r$ slightly above the instability threshold: $M = 20$, $S = 20$.

Fig. 2c Unstable eigenfunctions $b = ib_i$, $v = v_r$ for $S = M = 1000$.

Fig. 2d Unstable eigenfunctions $b = ib_i$, $v = v_r$ for $S = 10$, $M = 10^5$.

Fig. 2e Unstable eigenfunctions $b = ib_i$, $v = v_r$ for $S = 10^5$, $M = 10$.

Fig. 3 Highly damped complex eigenfunctions for $M = S = 20$.

Fig. 4 Locus of critical Reynolds-like numbers $S = S_c$, $M = M_c$ in the MS plane, as determined by computation.

Fig. 5 The neutral stability curve $\omega = 0$ in the α, S plane for $M = 1$, 10, and 1000 for B_o^{II} and $\gamma = 10$.

Fig. 6a Growth rates (ω_i vs. S) for $\alpha = 1.0$, (on B_o^{II} with $\gamma = 10$), $M = 10$, 100, and 1000.

Fig. 6b Growth rate ω_i vs. S for fixed M, $\alpha = 1.0$, B_o^{II} with $\gamma = 10$.

Fig. 7 Growth rate ω_i vs. M for fixed $S = 10$, 100, 1000; $\alpha = 1.0$, $\gamma = 10$ on B_o^{II}.

Fig. 8a Contour plot of magnetic field lines for a typical unstable eigenfunction near the threshold (S = M = 20). Field lines are equilibrium plus 20 percent admixture of eigenfunction.

Fig. 8b Velocity streamlines corresponding to eigenfunction represented in Fig. 8a.

Fig. 9 Growth rate ω_i vs. parallel wave number α for B_o^{II}, M = S = 100; M = S = 500; M = 1000, S = 100; M = 100, S = 1000.

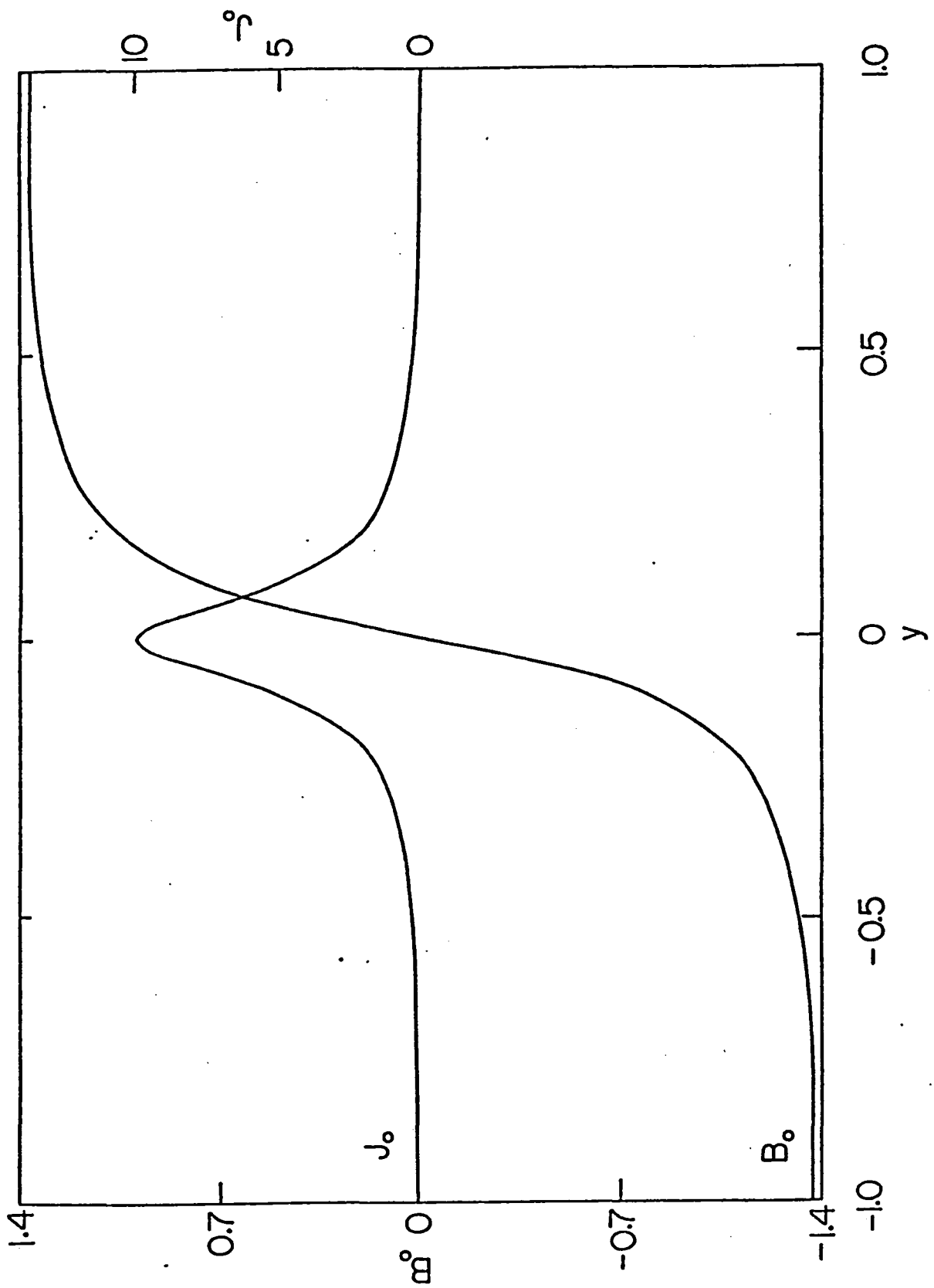

Fig. 1 $B_o = B_o^{II}(y)$ and its associated current profile $J_o = -DB_o$, for $\gamma = 10$.

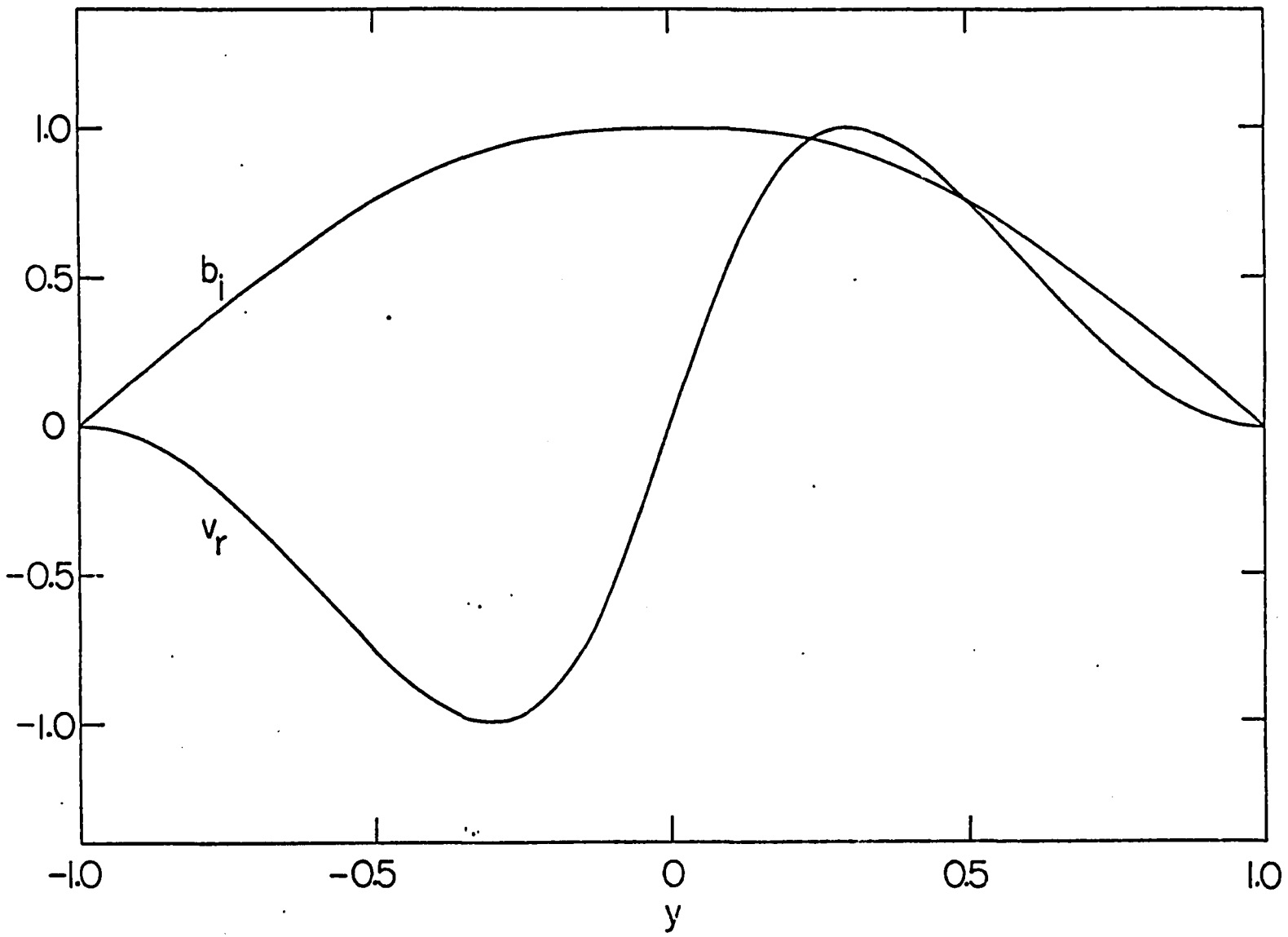

Fig. 2a Eigenfunctions $b = ib_i$, $v = v_r$ for the least-damped eigenvalues for M = 10, S = 10.

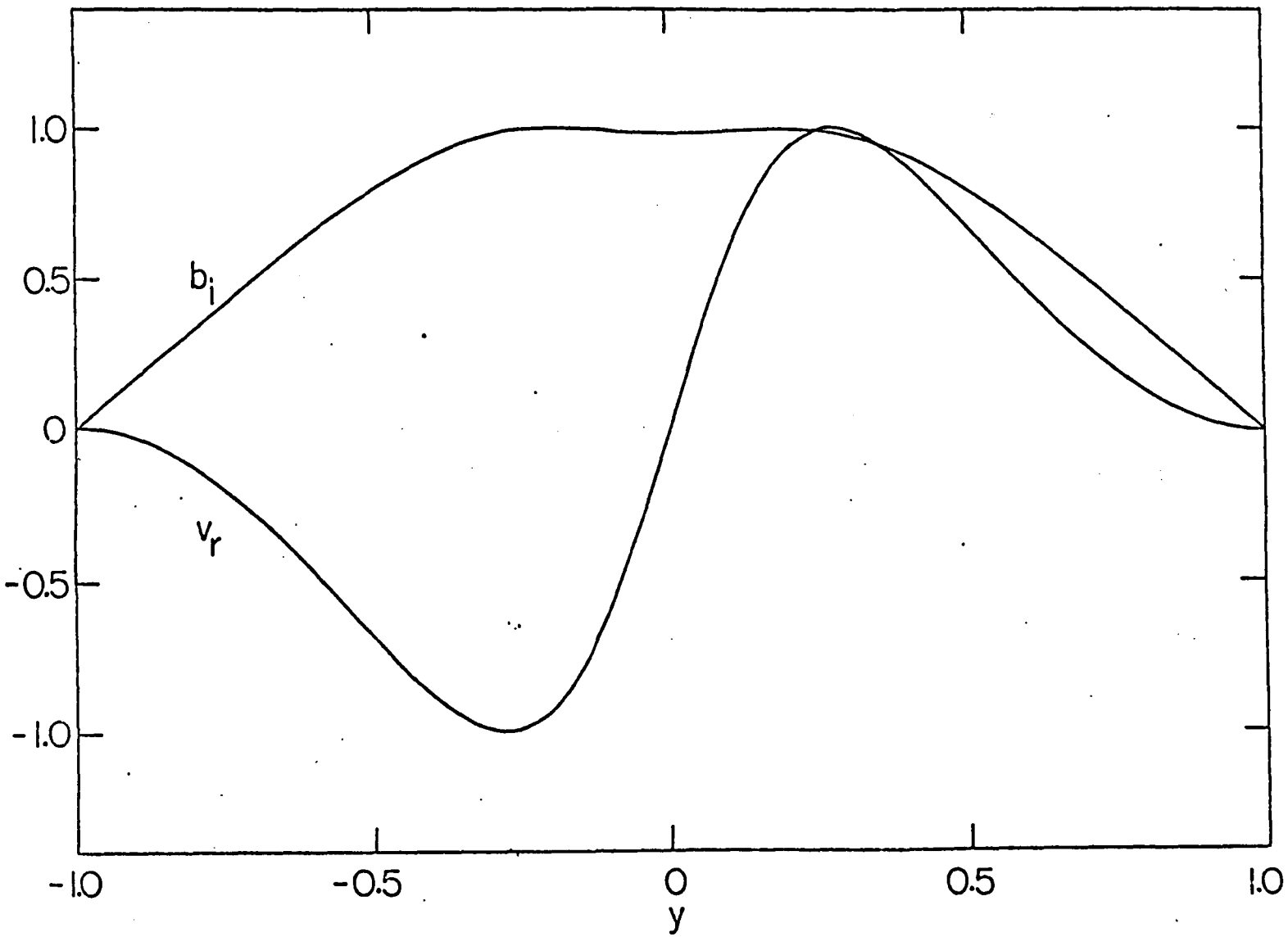

Fig. 2b Eigenfunctions $b = ib_i$, $v = v_r$ slightly above the instability threshold: M = 20, S = 20.

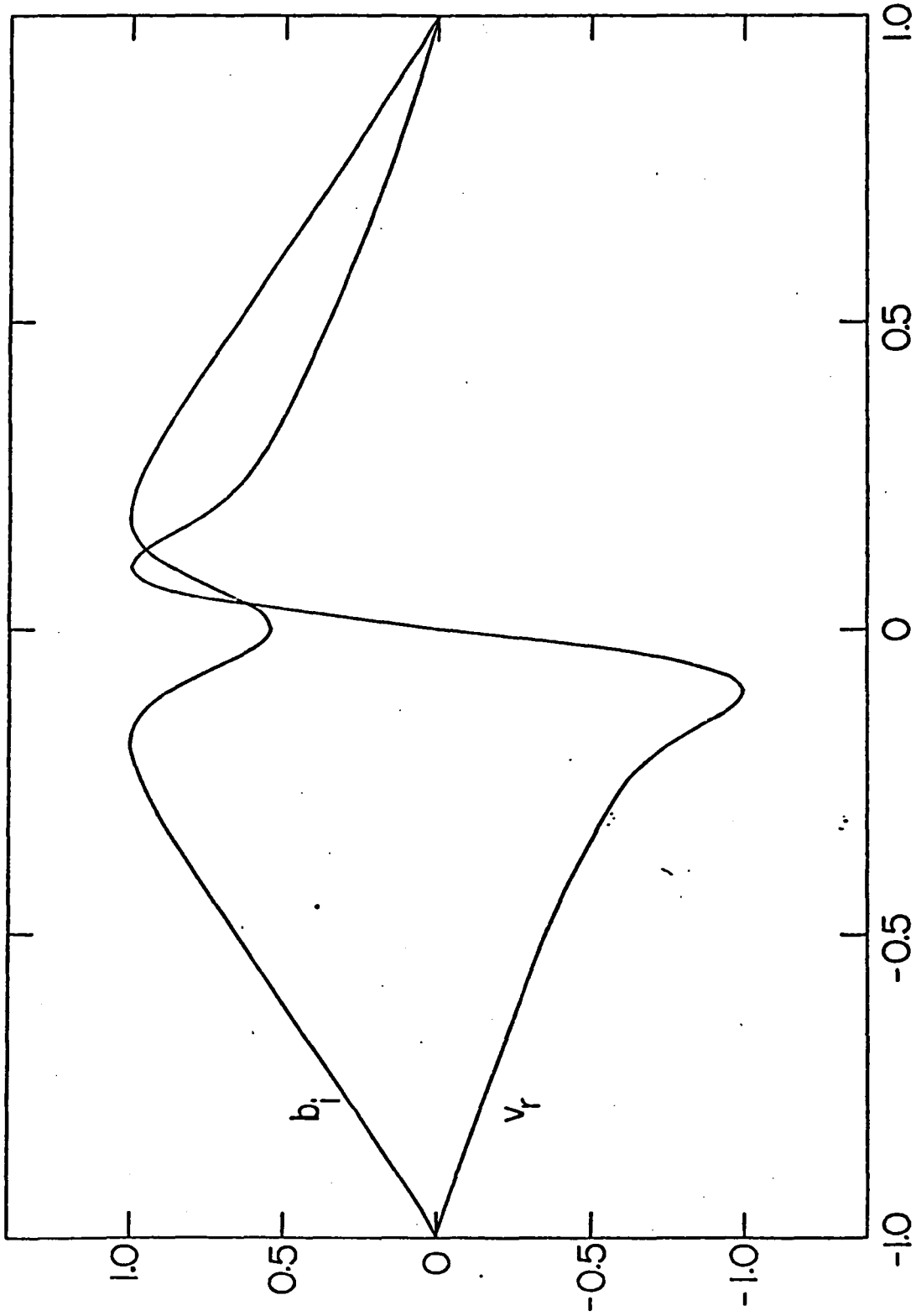

Fig. 2c Unstable eigenfunctions $b = ib_i$, $v = v_r$ for $S = M = 1000$.

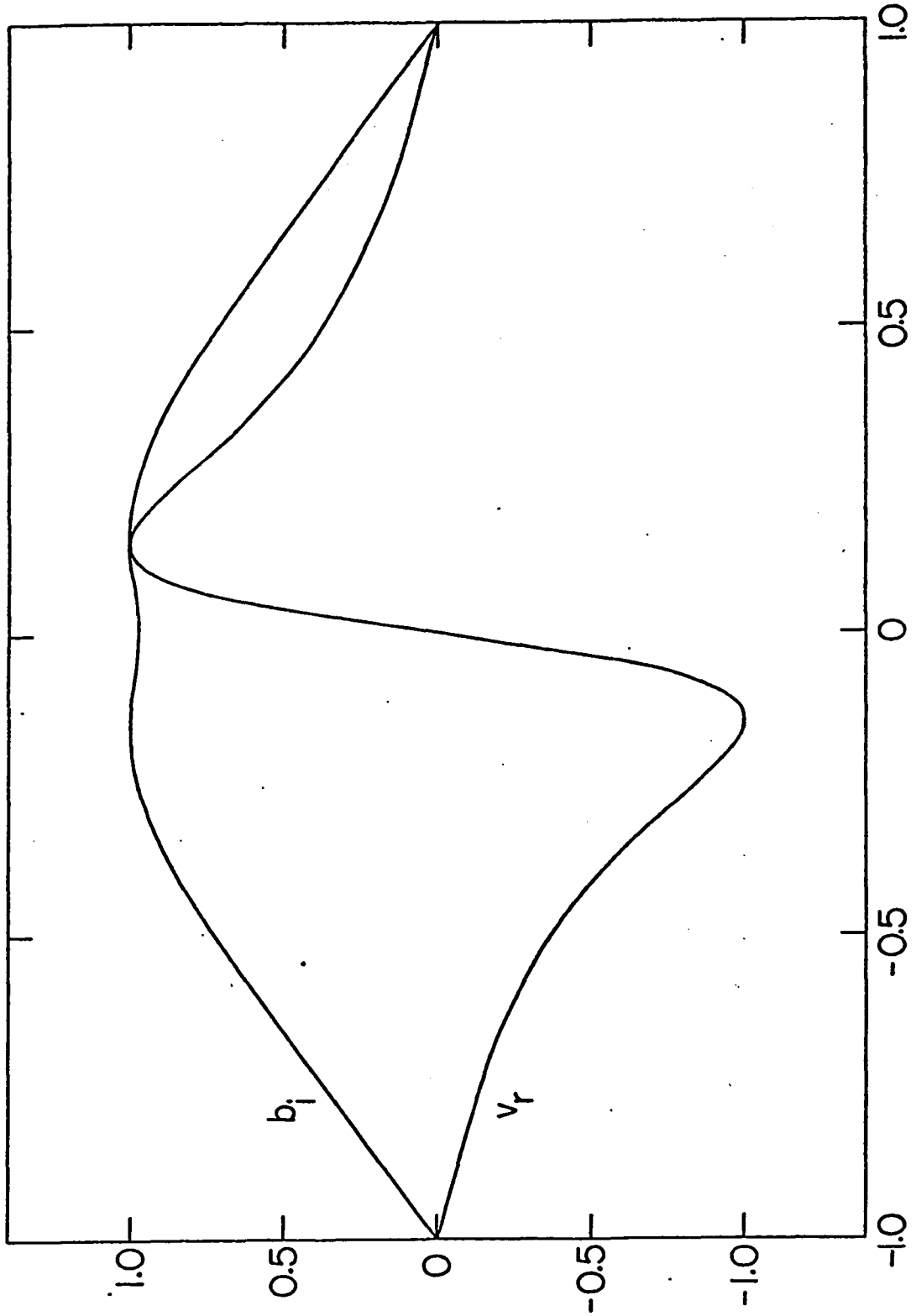

Fig. 2d Unstable eigenfunctions $b = ib_i$, $v = v_r$ for $S = 10$, $M = 10^5$.

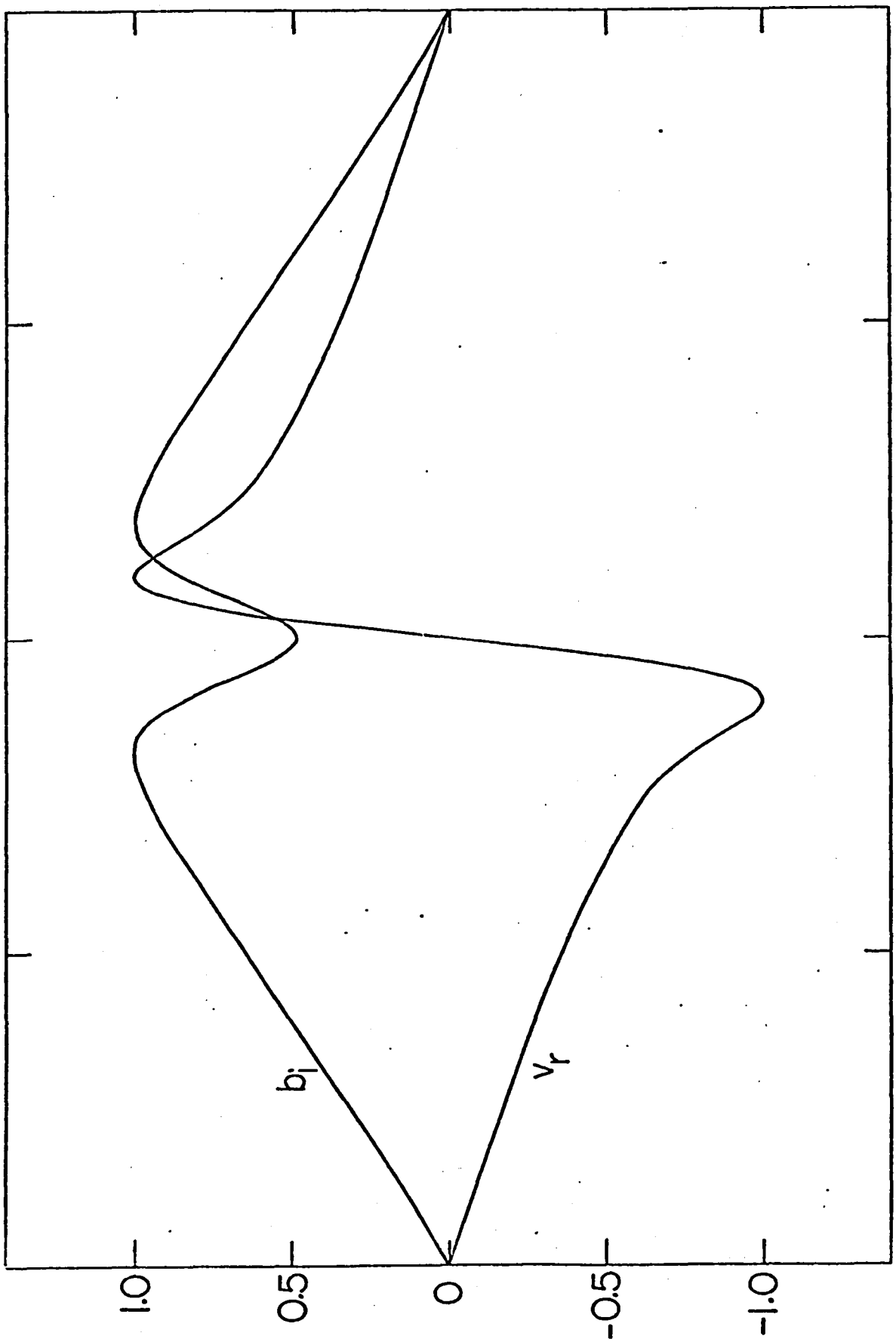

Fig. 2e Unstable eigenfunctions $b = ib_i$, $v = v_r$ for $S = 10^5$, $M = 10$.

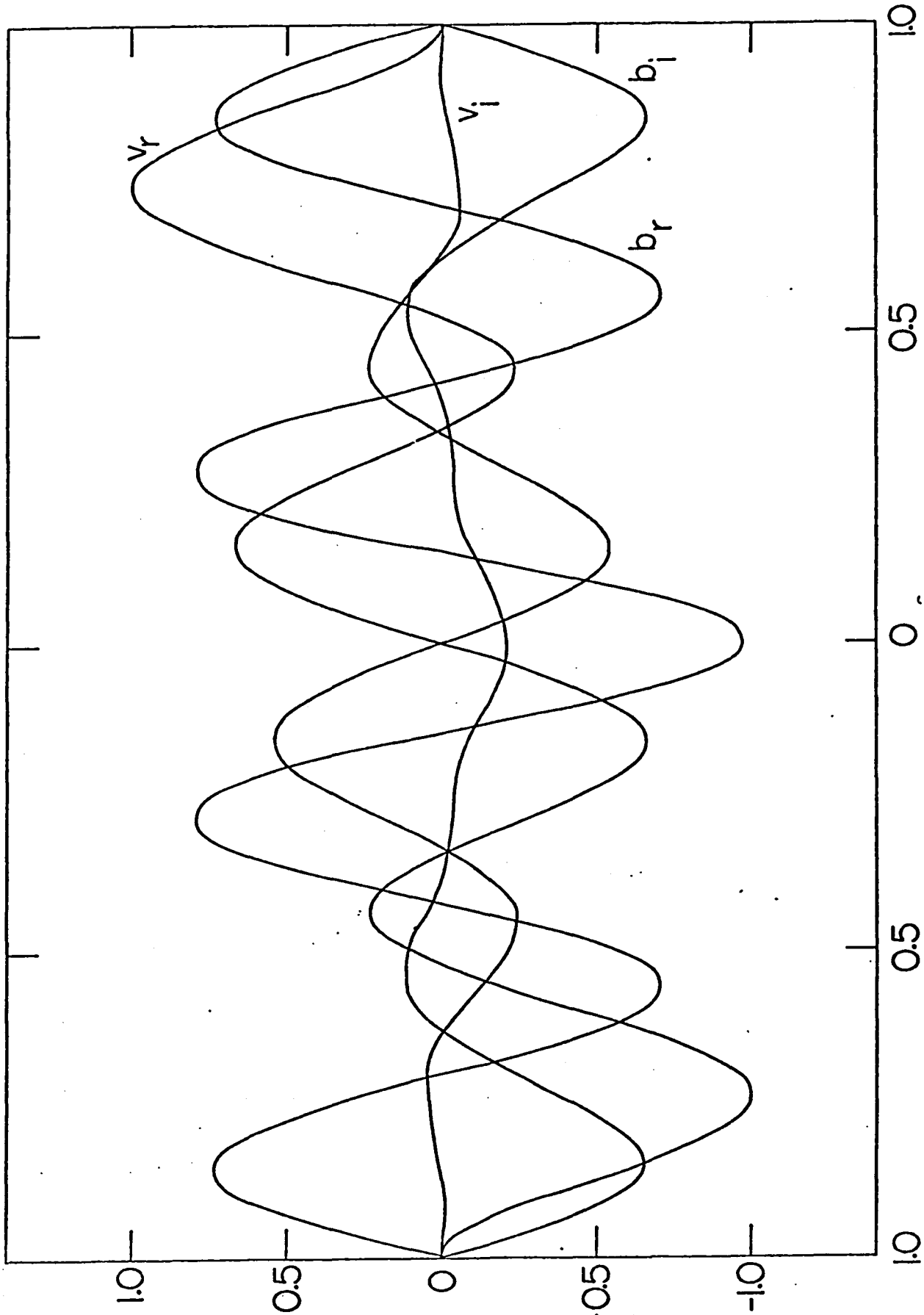

Fig. 3 Highly damped complex eigenfunctions for M = S = 20.

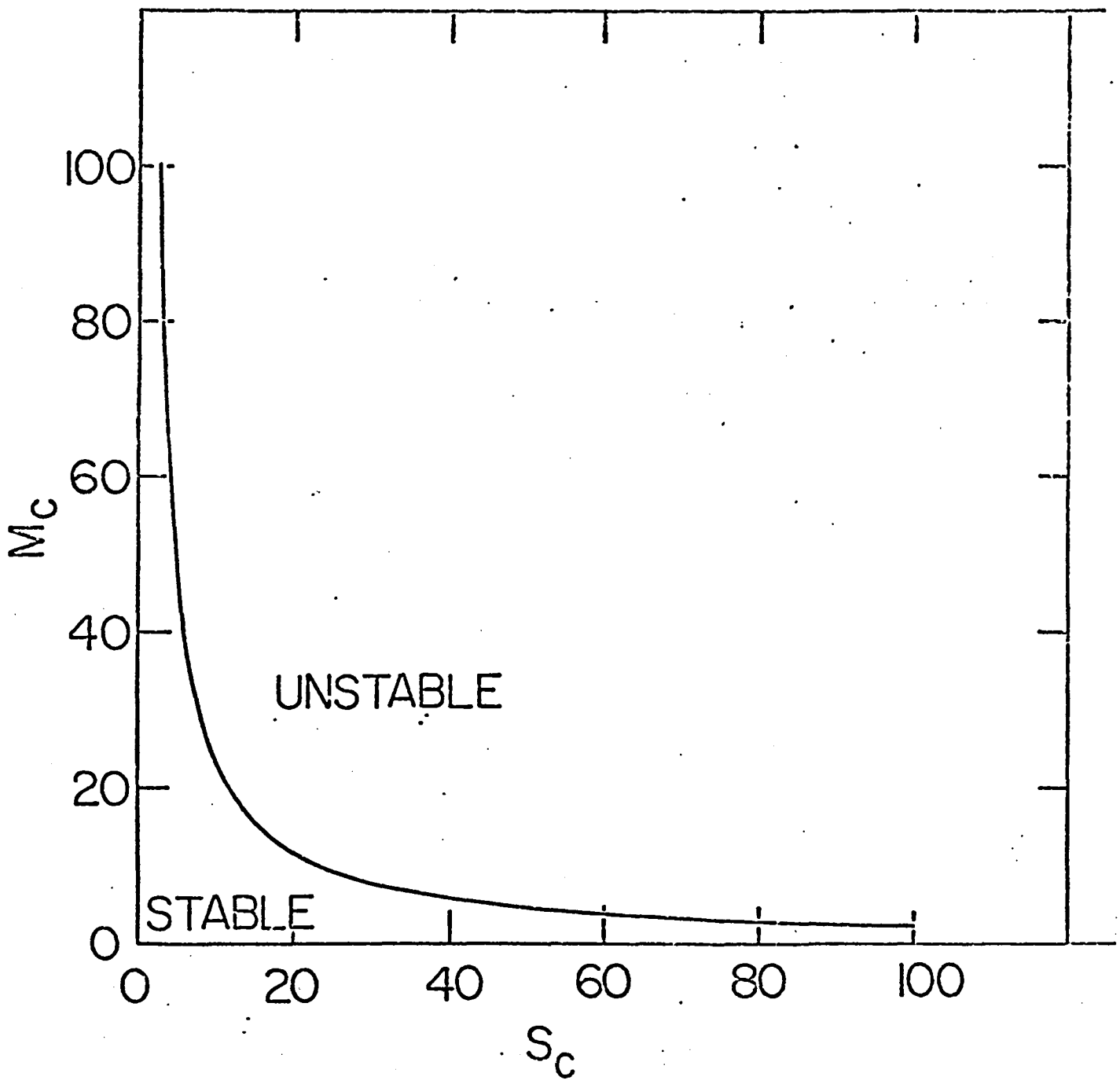

Fig. 4 Locus of critical Reynolds-like numbers $S = S_c$, $M = M_c$ in the MS plane, as determined by computation.

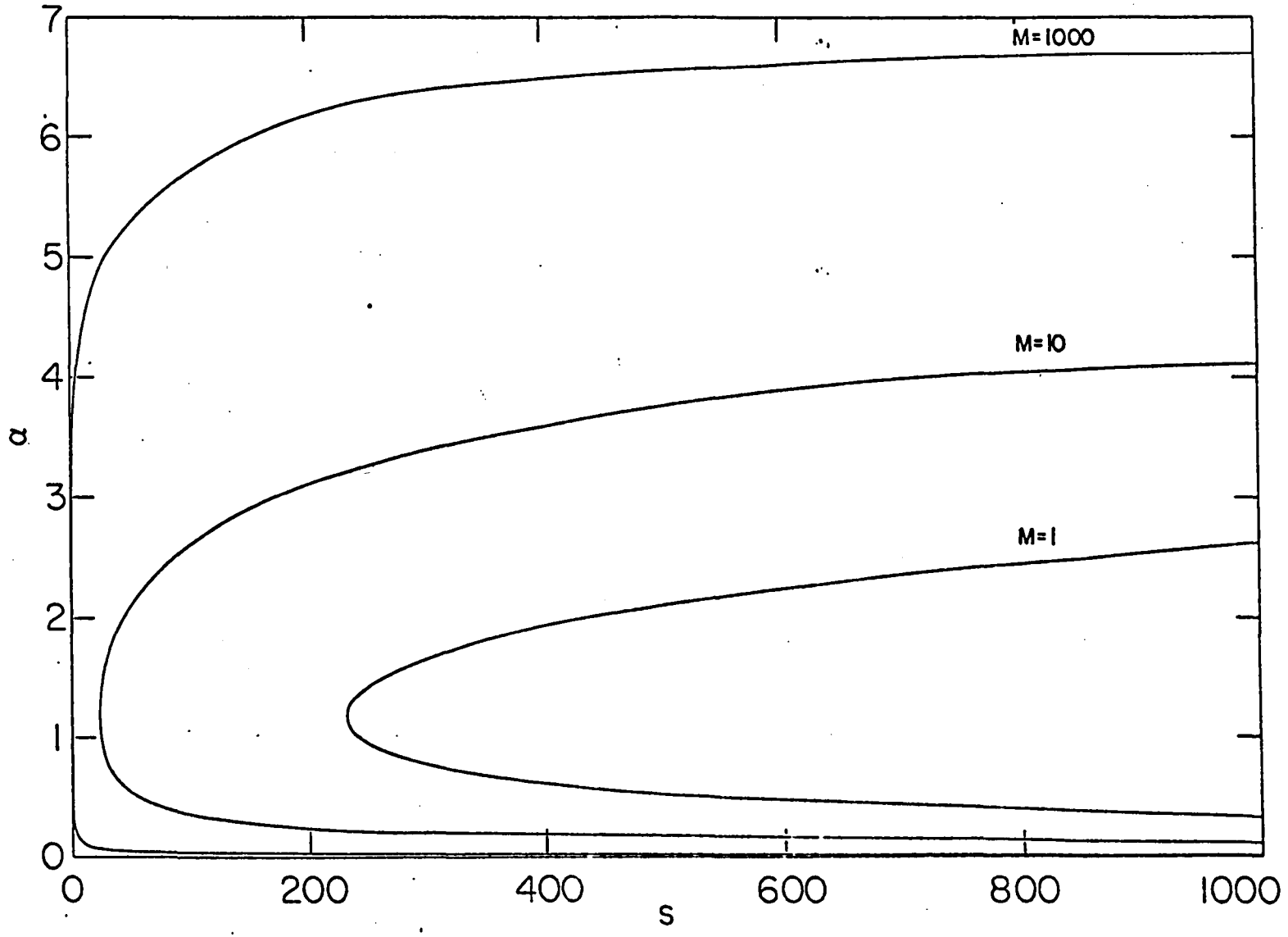

Fig. 5 The neutral stability curve $\omega = 0$ in the α, S plane for M = 1, 10, and 1000 for B_o^{II} and γ = 10.

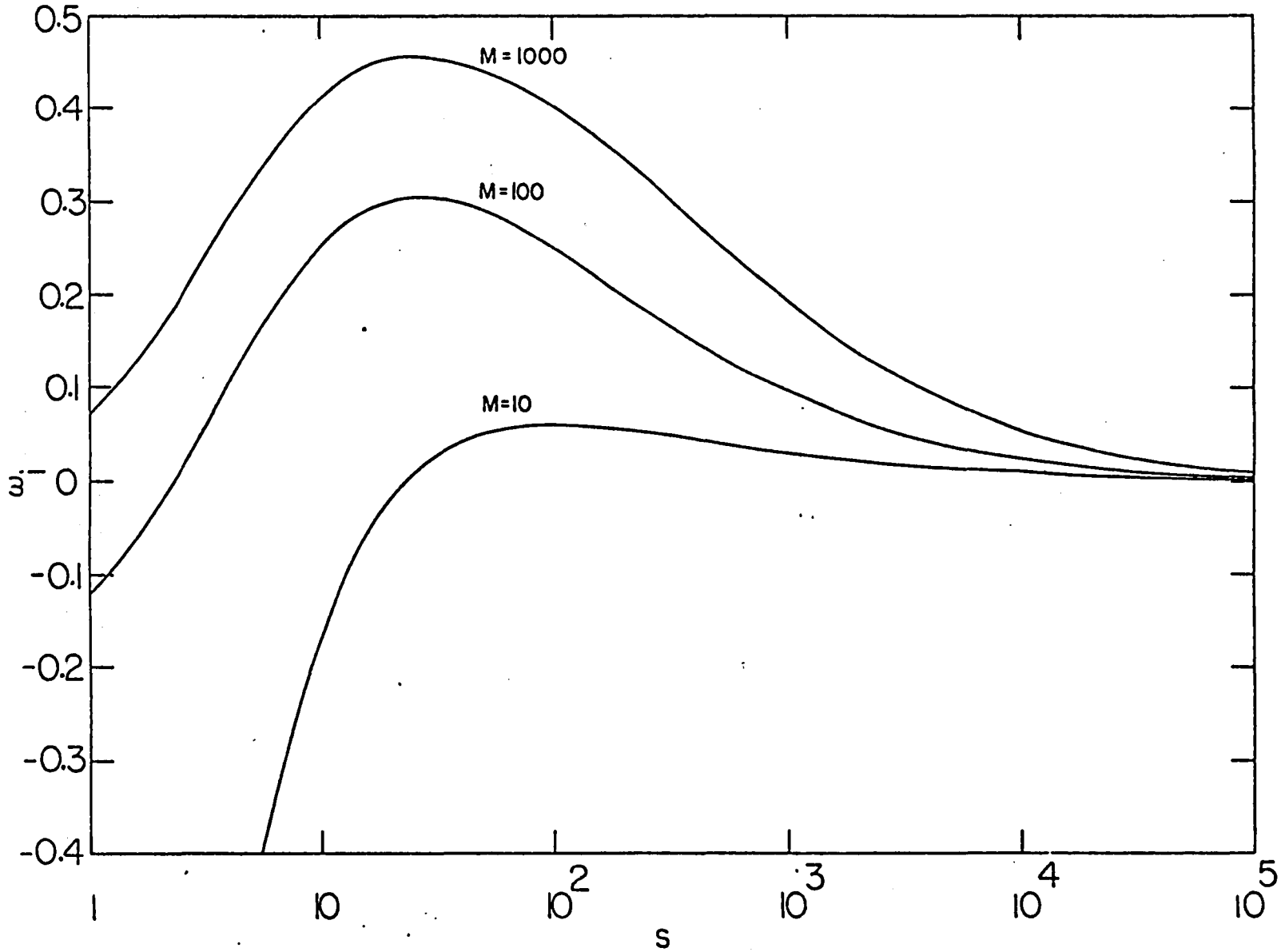

Fig. 6a Growth rates (ω_i vs. S) for $\alpha = 1.0$, (on B_o^{II} with $\gamma = 10$), M = 10, 100, and 1000.

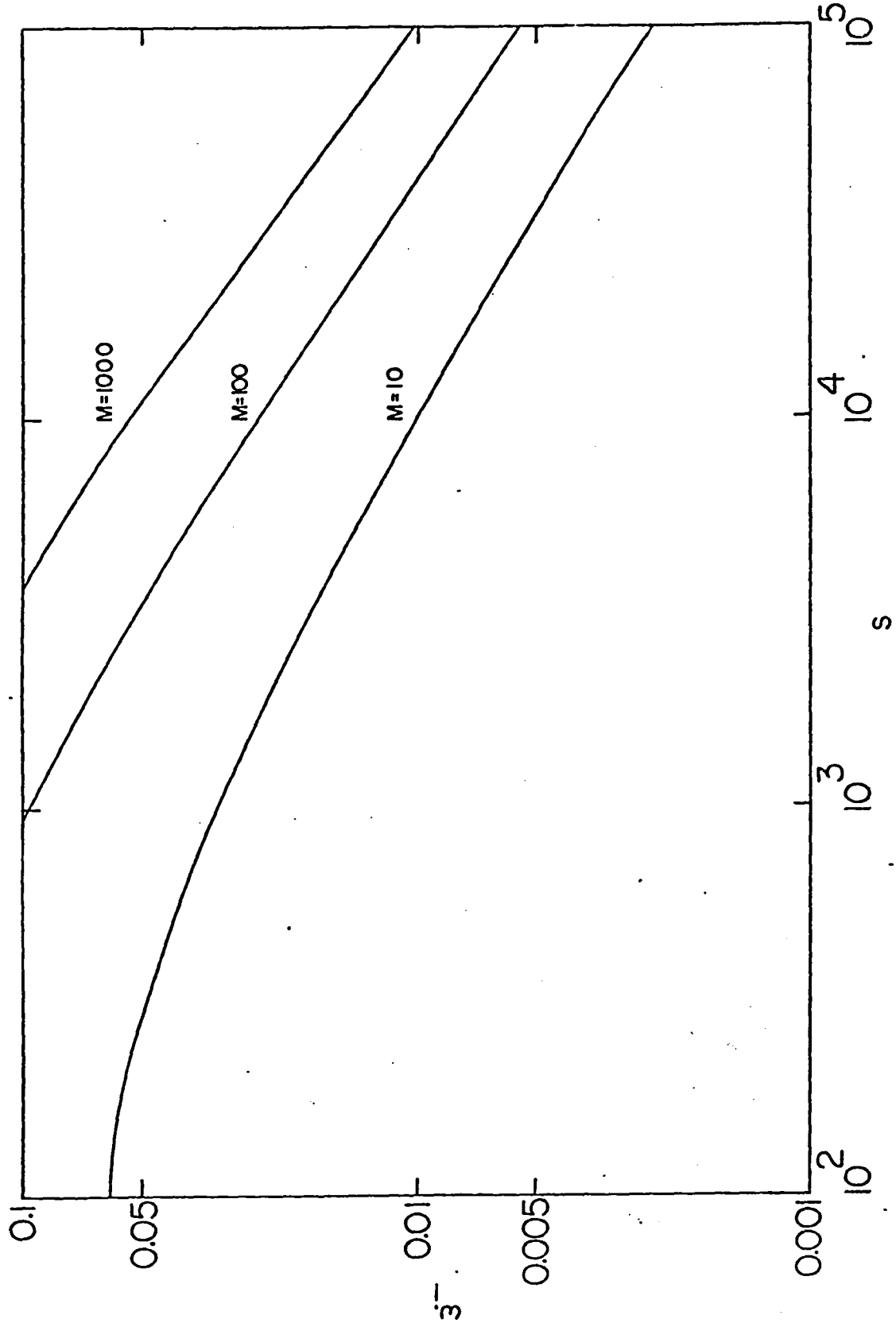

Fig. 6b Growth rate ω_1 vs. S for fixed M, $\alpha = 1.0$, B_o^{II} with $\gamma = 10$.

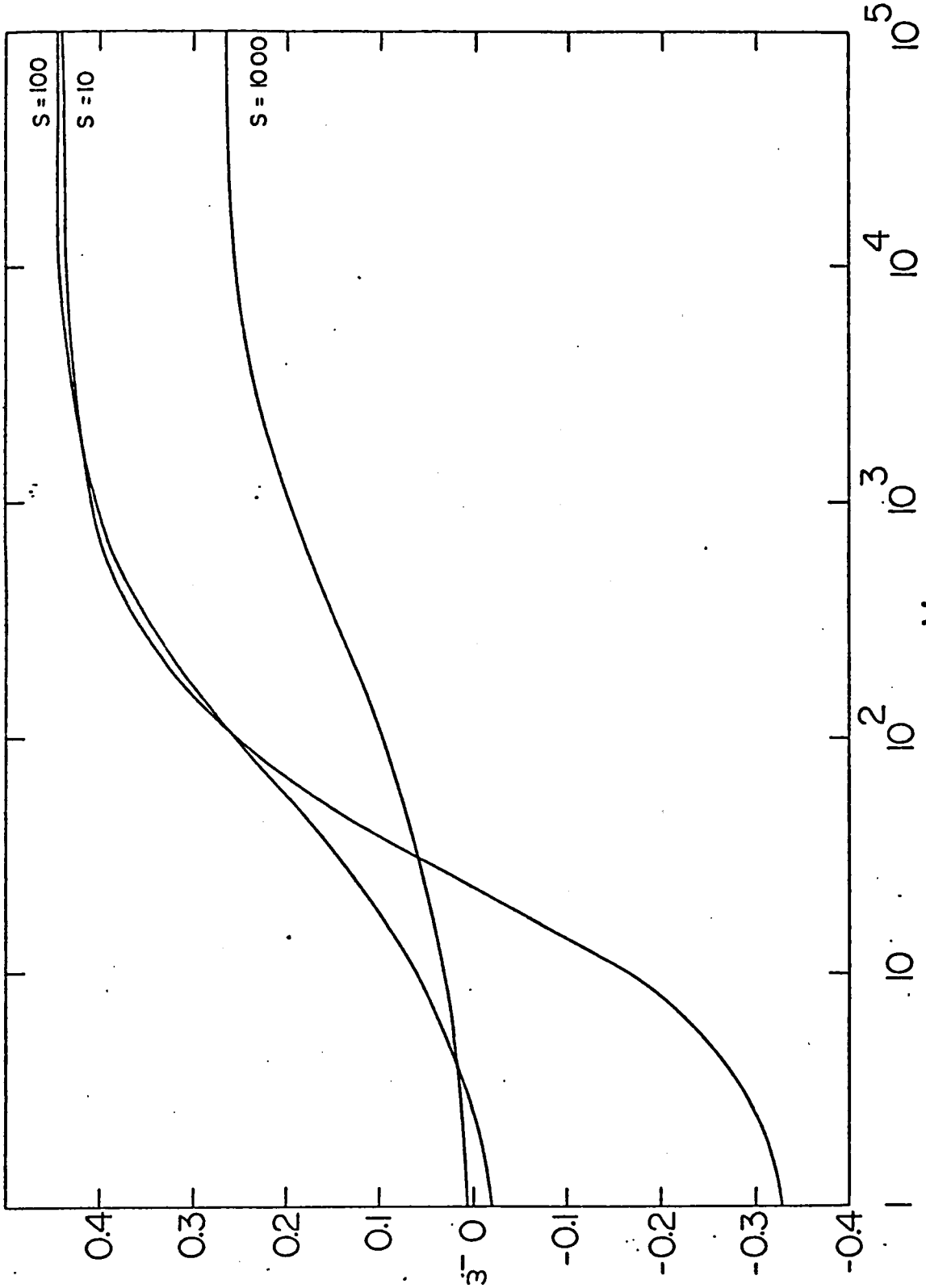

Fig. 7 Growth rate ω_i vs. M for fixed S = 10, 100, 1000; α = 1.0, γ = 10 on B_o^{II}.

Fig. 8a Contour plot of magnetic field lines for a typical unstable eigenfunction near the threshold (S = M = 20). Field lines are equilibrium plus 20 percent admixture of eigenfunction.

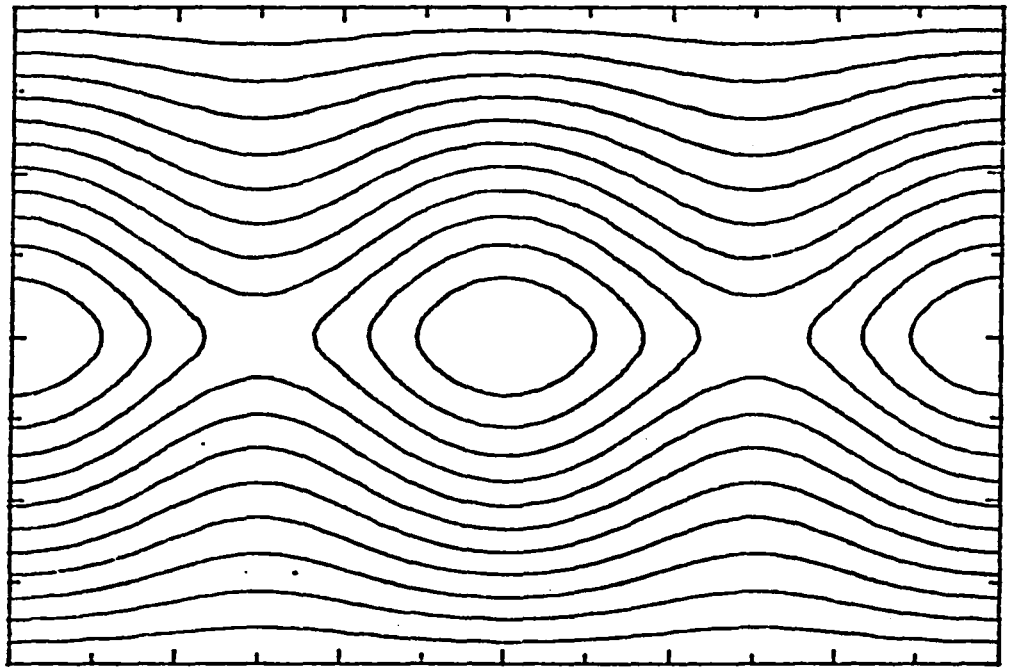

Fig. 8b Velocity streamlines corresponding to eigenfunction represented in Fig. 8a.

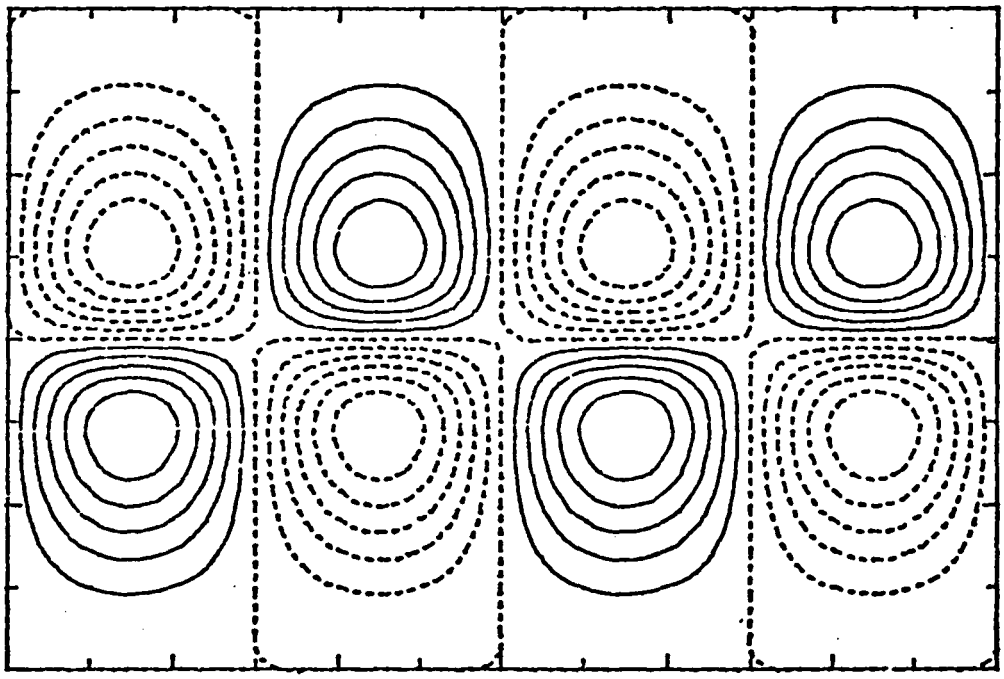

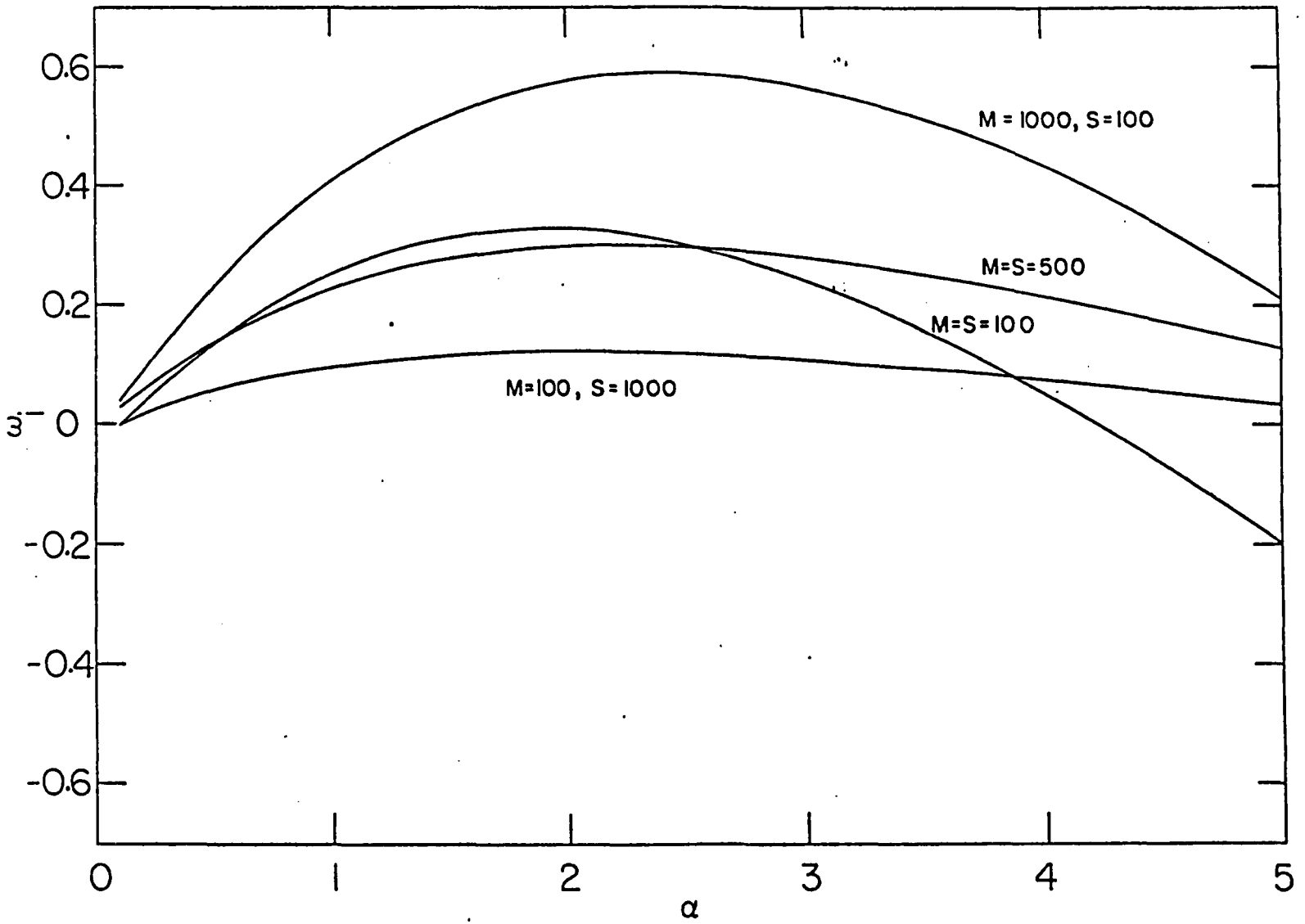

Fig. 9 Growth rate ω_i vs. parallel wave number α for B_o^{II}, M = S = 100; M = S = 500; M = 1000, S = 100; M = 100, S = 1000.

1. Report No.	2. Government Accession No.	3. Recipient's Catalog No.
NASA CR-172129		

4. Title and Subtitle	5. Report Date
VISCOUS, RESISTIVE MHD STABILITY COMPUTED BY SPECTRAL TECHNIQUES	March 1983
	6. Performing Organization Code
7. Author(s)	8. Performing Organization Report No.
R. B. Dahlburg, T. A. Zang, D. Montgomery, M. Y. Hussaini	83-3
	10. Work Unit No.
9. Performing Organization Name and Address	11. Contract or Grant No.
Institute for Computer Applications in Science & Engineering Mail Stop 132C, NASA Langley Research Center Hampton, VA 23665	NAS1-15810, NAS1-16394, NAG-1-109, NSG-7416
	13. Type of Report and Period Covered
12. Sponsoring Agency Name and Address	contractor report
National Aeronautics and Space Administration Washington, DC 20546	14. Sponsoring Agency Code

15. Supplementary Notes

Langley technical monitor: Robert H. Tolson
Final report

16. Abstract

Expansions in Chebyshev polynomials are used to study the linear stability of one-dimensional magnetohydrodynamic (MHD) quasi-equilibria in the presence of finite resistivity and viscosity. The method is modeled on the one used by Orszag in accurate computation of solutions of the Orr-Sommerfeld equation. Two Reynolds-like numbers involving Alfvèn speeds, length scales, kinematic viscosity, and magnetic diffusivity govern the stability boundaries, which are determined by the geometric mean of the two Reynolds-like numbers. Marginal stability curves, growth rates versus Reynolds-like numbers, and growth rates versus parallel wave numbers are exhibited. A numerical result which appears general in that instability has been found to be associated with inflection points in the current profile, though no general analytical proof has emerged. It is possible that nonlinear subcritical three-dimensional instabilities may exist, similar to those in Poiseuille and Couette flow.

17. Key Words (Suggested by Author(s))	18. Distribution Statement
MHD stability, Spectral Methods, Linear Theory	Unclassified-Unlimited Subject Category 75

19. Security Classif. (of this report)	20. Security Classif. (of this page)	21. No. of Pages	22. Price
Unclassified	Unclassified	29	A03

End of Document